Influence of the spatial structure on the effective nutrient diffusion in bacterial biofilm

T. Guélon, Jean-Denis Mathias, G. Deffuant

Author created version of the paper published in Journal of Biological Physics, Sept 2012, Volume 38, Issue 4, pp 573-588
Original publication available at http://link.springer.com, DOI: 10.1007%2Fs10867-012-9272-x

Influence of the spatial structure on the effective nutrient diffusion in bacterial biofilm

T. Guélon*[1], J.-D. Mathias[1], G. Deffuant[1]

[1] Cemagref - LISC (Laboratory of engineering for complex systems)
24, avenue des Landais - BP 50 085 - 63 172 Aubière Cedex 1 - France

* Corresponding author, Tel: +33 473440683
E-mail address: thomas.guelon@cemagref.fr (Thomas Guélon)

Author created version of the paper published in Journal of Biological Physics, Sept 2012, Volume 38, Issue 4, pp 573-588
Original publication available at http://link.springer.com, DOI: 10.1007%2Fs10867-012-9272-x

Abstract:

The main contribution of this paper is to use homogenization techniques to compute diffusion coefficients from experimental images of microbial biofilms. Our approach requires to analyze several experimental spatial structures of biofilms in order to derive from them a Representative Volume Element (RVE). Then, we apply a suitable procedure on the obtained RVE to compute the diffusion coefficients. We show that diffusion coefficients significantly vary with the biofilm structure. These results suggest that microbial biofilm structures can favour the nutrient access in some cases.

Keywords: homogenization techniques, diffusion process, nutrient access, bacterial biofilms.

Author created version of the paper published in Journal of Biological Physics, Sept 2012, Volume 38, Issue 4, pp 573-588
Original publication available at http://link.springer.com, DOI: 10.1007%2Fs10867-012-9272-x

1. Introduction

In natural, industrial and clinical settings, bacteria predominantly live in surface-associated communities called biofilm (Costerton et al., 1995). These biofilms, like other bacterial communities, have an important function in many industrial fields such as wastewater treatment (Daims et al., 2000), problem of biocorrosion (Beech and Sunner, 2004), biotechnology (Tijhuis et al., 1994; Wanner and Reichert, 1996) or medical science (Donlan and Costerton, 2002; Stewart and Costerton, 2001). In many industrial processes, the solute transport constitutes a key-issue in order to determine their performance. Solutes are mainly transported in bacterial biofilms by a combination of advection, convection and diffusion. However, molecular diffusion is the main mode of mass transport within bacterial biofilms (De Beer et al., 1994, 1997). A diffusion process can be completely defined by the assessment of the effective diffusion tensor D_{eff} that characterizes the diffusion process in all directions.

Different experimental studies highlight these diffusion phenomena, often with the aim to evaluate the effective diffusion and to understand its impact on bacterial biofilms. They have shown that different factors directly influence the nutrient diffusion such as the bacteria strain, the reactivity of the solutes or the density of bacteria for example. Different bacteria strains have been used such as *E. coli* (Libicki et al., 1988), *Z. ramigera* (Beyenal and Tanyolac, 1994). The intrinsic cell density varies from a bacteria strain to another and therefore drastically affects the calculation of the effective diffusion. For instance, the intrinsic cell density for *E. coli* is less important than the intrinsic cell density for *Z. ramigera* (Bakken and Olsen, 1983; Bratbak and Dundas, 1984) and conduct to a lower value of the effective diffusion. The reactivity of solutes has also been studied in order to evaluate its influence on the diffusion process. Matson and

Author created version of the paper published in Journal of Biological Physics, Sept 2012, Volume 38, Issue 4, pp 573-588
Original publication available at http://link.springer.com, DOI: 10.1007%2Fs10867-012-9272-x

Characklis (Matson and Characklis, 1976) have studied the diffusion of glucose through microbial aggregates under various experimental conditions. Methanol solutes (La Cour Jansen and Harremoes, 1985) or lactate (Dibdin, 1981) solutes have also been used to determine the effective diffusion of biofilms. The main conclusion is that the reactivity of the solute has an important influence on the diffusion process because some solutes can cross cell membranes and diffuse within the cell while others can be excluded by the cell membrane (see (Stewart, 1998) for a review of the different experimental measurements of the effective diffusion coefficient).

Predicting diffusion processes constitute a major industrial and scientific issue. Lamotta (Lamotta, 1976) has developed a theoretical model describing diffusion of substrate within the film matrix. He computed the effective diffusivity of glucose in biological films and showed that the fraction of substrate consumed is directly proportional to the film thickness, when thickness is less than a critical value. These different works determine the effective diffusion in biofilms and the influence of microscopic structures on the macroscopic behavior of the biofilm (Ochoa et al., 1986; Ochoa-Tapia et al., 1994; Wood et al., 2001, 2002). The effective diffusion coefficient is generally assumed to be a function of both the microscopic diffusions of the extra polysaccharide matrix and the cell aggregates (Gujer and Wanner, 1990). The conclusion of several papers is that microscopic parameters play an important role on the macroscopic properties of the biofilm, especially diffusion (Wood et al., 2001, 2002).

Bacterial biofilms show very complex heterogeneous structures (Jefferson, 2004; Roszak and Colwell, 1987), which are most probably related to their performances in the different industrial processes. Therefore, effective diffusion of biofilm is assumed to be a function of both microscopic diffusion and microstructure (Fan et al., 1990; Gujer and Wanner, 1990). In the last decades, the microscope gave access to the 2D and 3D observations of biofilm structures such as regular aggregates (Pamp and Tolker-Nielsen, 2007; Thar and Kuhl, 2005), mushroom shapes

Author created version of the paper published in Journal of Biological Physics, Sept 2012, Volume 38, Issue 4, pp 573-588
Original publication available at http://link.springer.com, DOI: 10.1007%2Fs10867-012-9272-x

(Allesen-Holm et al., 2006; Rieu et al., 2008), holes or labyrinths (Xavier et al., 2009). Moreover, new techniques have been coupled with microscope such as fluorescent microscopy (Xavier et al., 2009) that shows the location and evolution of bacteria strains in the whole biofilm. The freeze substitution technique (Hunter and Beveridge, 2005) also provides images of the biofilm in its original state and with finer structural details than a classical confocal microscope. These techniques give new means for observing bacteria local behaviours, the detachment process and bacteria competition.

The aim of this study is to show the influence of the spatial structures on the diffusion properties of bacterial biofilms. For this purpose, we use a suitable coupling between homogenization techniques and experimental images to compute the effective diffusion of biofilms. The first part of the paper is dedicated to the description of the experimental set-up in order to obtain experimental images. These images have been captured from a previous study (Xavier et al., 2009), and are then used to get typical structures which can be found within microbial biofilms. The second part of the paper is devoted to homogenization techniques. These techniques applied on these experimental images allow us to evaluate the macroscopic nutrient diffusion. They imply to define a representative volume element (RVE) and to run a suitable coupling between experimental images of biofilm and a finite element (FE) software. Finally, the paper focuses on results and on the impact of the spatial structure on the effective diffusion.

2. Materials and Method

2.1 Experimental set-up

We use the biofilm images from the paper of Xavier & al. (Xavier et al., 2009), which proposes a model of cell growth at a surface, to fit the development of *Pseudomonas aeruginosa*. The experimental setting consists in cultivating a biofilm on glass coverslip submerged in

Author created version of the paper published in Journal of Biological Physics, Sept 2012, Volume 38, Issue 4, pp 573-588
Original publication available at http://link.springer.com, DOI: 10.1007%2Fs10867-012-9272-x

inoculated liquid medium. This setup was incubated for 24h at room temperature in the absence of any agitation. Then, the coverslip was extracted and a robust biofilm was visible. Fluorescent microscopy of fluorescent protein-labelled biofilm has shown cells in spatial patterns with holes, labyrinths or worm-like shapes. The paper investigates how evolutionary competition among individuals affects the biological organization. Indeed, the authors highlighted that a competition between growth and nutrients competition can explain how observed spatial structures emerge in biofilms. Their contribution is to provide a formal link between higher level patterning and the potential for evolutionary conflict in social systems. The typical spatial structures of biofilms obtained in (Xavier et al., 2009) are represented in Figure 1. Three types of structures can be distinguished: "worm-like" (Figure 1-a), "labyrinth" (Figure 1-b) and "dense" (Figure 1-c).

These three configurations have experimentally been obtained by varying the nutrient concentration. These images are continuous in time. The "worm-like" configuration is obtained at the beginning of the experience when cells begin to colonize the surface; the nutrient competition between cells is very important due to a limited substrate. The biofilm growth is therefore limited and small colonies form the biofilm. If we increase the substrate concentration, nutrient competition is less important between bacteria, growth becomes heterogeneous in space, circular colonies deform due to fingering (Dockery and Klapper, 2002; Xavier et al., 2009) and leads to the "labyrinth" configuration. Conversely, if the nutrient concentration is saturated, all bacteria have a nutrient access, the nutrient competition is less important; the biofilm growth is fast until reaching the "dense" configuration.

The aim of this work is to evaluate the influence of these spatial structures on the effective nutrient diffusion and to give new means on the competition between growth and nutrient access. For this purpose, we use homogenization techniques on these experimental images.

Author created version of the paper published in Journal of Biological Physics, Sept 2012, Volume 38, Issue 4, pp 573-588
Original publication available at http://link.springer.com, DOI: 10.1007%2Fs10867-012-9272-x

2.2 Homogenization techniques

2.2.1 Principle

The main purpose of homogenization techniques is to compute macroscopic properties from microscopic properties. These techniques have been successfully addressed in several applications, especially in mechanics (Hashin, 1983; Mathias and Tessier-Doyen, 2008). Homogenization techniques allow us to scale of physical quantities from the microscale to the macroscale. Generally, continuum mechanics deals with the evolution of continuous material systems in two or three dimensions and time. One of the most critical elements of the continuum approach is the concept of representative volume element (RVE). The RVE is an infinitesimal part of the considered system. More precisely, if we denote by L and l the characteristic lengths of respectively the structure and the RVE, the condition $l << L$ guarantees the relevance of differential calculus. Furthermore, the RVE is expected to be large enough to be representative of the constitutive media.

This property requires the characteristic size l of the RVE to capture the geometrical and physical properties of the system. Indeed, if we denote d, the characteristic length scale of the local heterogeneities, typically the cell size in a bacterial biofilm, the condition $d << l$ is expected to ensure that the elementary volume is representative. In summary, the two conditions on the size of the RVE are (see Figure 2):

$$d << l << L \tag{1}$$

Relation 1 is often referred as the scale separation condition, which is a necessary condition for the concept of RVE to be valid. In order to compute appropriate values of l we perform a convergence study by calculating the homogenized parameters following several RVE sizes.

Author created version of the paper published in Journal of Biological Physics, Sept 2012, Volume 38, Issue 4, pp 573-588
Original publication available at http://link.springer.com, DOI: 10.1007%2Fs10867-012-9272-x

2.2.2 Theoretical background

We model the diffusion process with the Fick law in two dimensions (experimental images are in two dimensions):

$$F = -D\nabla c \tag{2}$$

F corresponds to the diffusive flux vector expressed in mol.$\mu m^{-2}.s^{-1}$, D to the diffusion tensor expressed in $\mu m^2.s^{-1}$ and ∇c to the concentration gradient vector expressed in mol. μm^{-4}. In this study, we have considered a two-phase system consisting of bacteria (the σ-phase) in the domain Ω_σ and bulk liquid (the β-phase) in the domain Ω_β (see Figure 3). Then, the diffusion process follows the Fick law at the subcellular scale:

$$F_\sigma = -D_\sigma \nabla c_\sigma \quad in \Omega_\sigma \tag{3}$$

in the intercellular phase (σ-phase) and

$$F_\beta = -D_\beta \nabla c_\beta \quad in \Omega_\beta \tag{4}$$

in the extracellular phase (β-phase).

The idea is to calculate the effective diffusion D_{eff} of the domain Ω defined as follows:

$$F = -D_{eff} \nabla c \tag{5}$$

We define the volume average theorem considering that D_{eff} is independent of position:

$$< F >= -D_{eff} < \nabla c > \tag{6}$$

with

$$< F >= \int_{\Omega_\beta} F ds + \int_{\Omega_\sigma} F ds \tag{7}$$

$$< \nabla c >= \int_{\Omega_\beta} \nabla c ds + \int_{\Omega_\sigma} \nabla c ds \tag{8}$$

Then relevant boundary conditions are imposed in order to simplify these equations. These boundary conditions can be expressed in terms of homogeneous flux or homogeneous

Author created version of the paper published in Journal of Biological Physics, Sept 2012, Volume 38, Issue 4, pp 573-588
Original publication available at http://link.springer.com, DOI: 10.1007%2Fs10867-012-9272-x

concentration gradient. In the following, concentration gradients ∇c^{mac} are imposed at the boundary $\delta\Omega$ (see Figure 3). We obtain the relation between ∇c and c using the Gauss theorem:

$$\begin{aligned} \int_\Omega c_{,j} d\Omega &= \int_{\delta\Omega} c n_j dS \\ &= \nabla c^{mac} \int_{\delta\Omega} x_i n_j dS \\ &= \nabla c^{mac} \int_\Omega x_{i,j} d\Omega \\ &= |\Omega| \nabla c^{mac} \end{aligned} \tag{9}$$

It yields the following relationship between the microscopic concentration gradient ∇c and the macroscopic concentration gradient ∇c^{mac} with the average operator:

$$\begin{aligned} < \nabla c > &= \frac{1}{|\Omega|} \int_\Omega \nabla c d\Omega \\ &= \frac{1}{|\Omega|} \int_\Omega c_{,j} d\Omega \\ &= \nabla c^{mac} \end{aligned} \tag{10}$$

Finally, we can identify D_{eff} as follows:

$$\nabla c^{mac} D_{eff} = - < F > \tag{11}$$

In the following, we consider a two-dimensional problem depending on the *x*- and *y*-directions. In this case, the effective tensor D_{eff} writes as follows:

$$D_{eff} = \begin{pmatrix} d_{eff}^{xx} & d_{eff}^{xy} \\ d_{eff}^{xy} & d_{eff}^{yy} \end{pmatrix} \tag{12}$$

Note that in the case of an isotropic behavior, this tensor is diagonal, with $d_{eff}^{xx} = d_{eff}^{yy}$. However, in the general case, some couplings between the *x*- and *y*-directions may occur and it is necessary to calculate the complete effective diffusion matrix. Some analytical solutions have been developed in the literature in some simple cases (see Section 2.3). These analytical solutions will be used as reference solutions in the following. However, in the general case, it is not possible to apply these solutions: therefore we use a numerical resolution.

Author created version of the paper published in Journal of Biological Physics, Sept 2012, Volume 38, Issue 4, pp 573-588
Original publication available at http://link.springer.com, DOI: 10.1007%2Fs10867-012-9272-x

2.2.3 Numerical resolution

We use a numerical procedure to calculate the effective tensor of diffusion D_{eff} on the domain Ω. The experimental images constitute our representative volume element (RVE). The images are threshold, vectorized and imported on the finite element code Comsol 3.3, and then we perform the meshing. The geometry is discretized with 2D triangular elements (see Figure 4).

In order to determine D_{eff} (see Equation 12), it is necessary to perform two tests for the assessment of the effective diffusion coefficients (see Figure 5). For this purpose, we consider a square RVE (with the length of the side equal to l). For the first test, we impose: $c(L_1) = 0$, $c(L_2) = c(L_4) = \frac{a * x}{l}$, $c(L_3) = a$, leading to:

$$\nabla c_{test1}^{mac} = \begin{pmatrix} \frac{a}{l} \\ 0 \end{pmatrix} \tag{13}$$

For the second test, we impose: $c(L_1) = c(L_3) = \frac{a * y}{l}$, $c(L_4) = a$, $c(L_2) = 0$. It leads to:

$$\nabla c_{test2}^{mac} = \begin{pmatrix} 0 \\ \frac{a}{l} \end{pmatrix} \tag{14}$$

From these tests and using Equation 11, the components of the effective diffusion matrix are calculated as follows:

$$\begin{aligned} d_{eff}^{xx} &= \frac{l < F_{test1}^{x} >}{a} \\ d_{eff}^{yy} &= \frac{l < F_{test2}^{y} >}{a} \\ d_{eff}^{xy} &= \frac{l < F_{test1}^{y} >}{a} = \frac{l < F_{test2}^{x} >}{a} \end{aligned} \tag{15}$$

Author created version of the paper published in Journal of Biological Physics, Sept 2012, Volume 38, Issue 4, pp 573-588
Original publication available at http://link.springer.com, DOI: 10.1007%2Fs10867-012-9272-x

$< F^{i}_{testk} >$ corresponds to the numerical integration of the component i of the vector F for the k^{th}-test. These numerical tests enable us to assess the effective diffusion matrix. In order to validate the current procedure and to highlight the influence of the spatial structure, analytical solutions are now presented for validating and comparing our approach.

2.3 Analytical Solutions

As explained in the introduction, different theoretical models have been developed in order to calculate the effective diffusion D_{eff}. These models are essentially based on the assumption of a uniform distribution of the bacteria. The influence of the spatial structure is neglected in this type of model which constitutes a mean field approximation of the effective diffusion in the case of a uniform distribution. In the following, we used the Maxwell's solution (Maxwell, 1891) which takes the form:

$$D_{eff} = \frac{2*D_\sigma + D_\beta + \rho*(D_\sigma - D_\beta)}{2*D_\sigma + D_\beta - 2*\rho*(D_\sigma - D_\beta)} * D_\beta \tag{16}$$

with

$$\rho = \frac{S_\sigma}{S_{tot}} \tag{17}$$

S_σ is the surface of the σ-phase and S_{tot} is the total surface of the domain. We can also referred to the Chang's unit cell (Chang, 1983) where the periodic assumption has been replaced by Dirichlet conditions:

$$D_{eff} = \frac{(1-\rho)*D_\beta + (1+\rho)D_\sigma}{(1-\rho)*\frac{D_\sigma}{D_\beta} + 1 + \rho} \tag{18}$$

These analytical solutions are used as reference solutions in order to validate the current approach and to highlight the influence of the spatial structure. Both analytical solutions can be

Author created version of the paper published in Journal of Biological Physics, Sept 2012, Volume 38, Issue 4, pp 573-588
Original publication available at http://link.springer.com, DOI: 10.1007%2Fs10867-012-9272-x

used in order to calculate effective parameters in two-phase media. They have already been used as reference solutions for effective diffusion in the case of bacterial biofilms (Wood and Whitaker, 1998; Wood et al., 2002).

3 Applications

3.1 VER convergence

Representative volume elements (RVE) have to be used for homogenization procedures. If the RVE size is too small, it will not be representative. If the RVE size is too big, it will be representative but the calculation time will be important. We perform a convergence study to determine the suitable size of the RVE. Moreover, we investigate the variation of the homogenized parameter, here, the effective diffusion, according to different RVE sizes. On Figure 6, we can see different sizes of RVE that we tested. The results obtained on the case of labyrinth configuration are presented in Figure 7 as an example. It shows the evolution of d_{eff}^{xx} following the surface of the RVE. The "min/max" bar enables us to characterize the scattering of the results which is directly linked to the representativeness of the RVE. Indeed, if the minimum value is close to the maximum value computed by the current procedure, all RVE lead to the same result. In this case, we can conclude that the RVE leads to a good representativeness of the volume. This phenomenon is clearly shown on Figure 7. The "min/max" bar is very important for small surfaces of RVE, and decreases with respect to the RVE surface. For small surfaces, it means that all RVE with this area have homogeneous properties. Moreover, the mean value converges for a RVE area superior to 10000 μm^2. In this configuration, i.e. labyrinth configuration, we can conclude that a domain with a size of 100 µm by 100 µm is representative. In the following, we have therefore performed calculations with a RVE area of 13000 μm^2 in order to completely minimize the scattering of the results. We performed the same study on the

Author created version of the paper published in Journal of Biological Physics, Sept 2012, Volume 38, Issue 4, pp 573-588
Original publication available at http://link.springer.com, DOI: 10.1007%2Fs10867-012-9272-x

two other configurations (dense and worm-like configurations) and we conclude the RVE is also representative with a area of 13000 μm^2 for both of them.

3.2 Calculation of the effective diffusion

Homogenization techniques are now applied on the three biofilm spatial structures that can be observed on Figure 1. For the tests described in section 2, we have used a=10 and l=114µm. The value of a has no influence on the results because of the linearity of the Fick equation (see Equation 2). The length l is directly deduced from the convergence study of the RVE, described in the precedent section.

Afterward, we have to choose the diffusion coefficient of the bacteria and of the bulk liquid. Within the bacteria, the diffusion process is limited whereas it is important in the bulk liquid. We have decided to impose a value D_σ of the diffusion within the bacteria equal to 1 $\mu m^2.s^{-1}$ and a value D_β of the diffusion in the bulk liquid equal to 100 $\mu m^2.s^{-1}$. The ratio between these two coefficients plays an important role and is analysed in section 3.3.

The idea is to perform the calculation in the case of a negligible diffusion within bacteria. Moreover, all following calculations depend on the microbial density. In this study, the microbial density varies according to the spatial configuration. Indeed, the density is equal to 0.97, 0.33, 0.17 for dense, labyrinth and worm-like configurations, respectively.

We have obtained the following diffusion tensor for the dense configuration:

$$D_{eff} = \begin{pmatrix} 1.13 & 0.015 \\ 0.017 & 1.13 \end{pmatrix} \mu m^2.s^{-1} \quad (19)$$

For the labyrinth configuration, calculations lead to:

$$D_{eff} = \begin{pmatrix} 29.94 & 0.15 \\ 0.18 & 27.16 \end{pmatrix} \mu m^2.s^{-1} \quad (20)$$

Finally, for the worm-like configuration, we have:

Author created version of the paper published in Journal of Biological Physics, Sept 2012, Volume 38, Issue 4, pp 573-588
Original publication available at http://link.springer.com, DOI: 10.1007%2Fs10867-012-9272-x

$$D_{eff} = \begin{pmatrix} 67.58 & 0.89 \\ 1.12 & 62.61 \end{pmatrix} \mu m^2.s^{-1} \quad (21)$$

In the case of "dense" configuration, the nutrient concentration is high. There is no nutrient competition between cells, the biofilm growth is therefore important and leads to a dense biofilm. Indeed, bacteria fill the whole domain; the microbial density (equal to 0.97) is almost maximal. Consequently, the effective diffusion is low and the diffusion process has a minor role. Note that the value of effective diffusion is close to the parameter of diffusion in the bacteria (D_σ = 1 $\mu m^2.s^{-1}$).

In the case of "worm-like" configuration, the nutrient concentration is limited. The nutrient competition between cells is very important and the growth condition is therefore unfavourable, small colonies form the biofilm. The bacteria density is low and leads to the higher value of the effective diffusion.

The case of "labyrinth" configuration is an intermediate step between both previous cases. The nutrient concentration is higher than the "worm-like" case, there is a nutrient competition between bacteria but the growth is heterogeneous in space. The phenomenon of fingering and the mechanical pushing lead to this "labyrinth" configuration. The value of effective diffusion is between the previous values. The substrate diffusion is facilitated along the direction created by both phenomena. However, the substrate diffusion remains lower than in the case of the worm-like configuration because of the spatial structure and of the higher bacteria density is higher.

It is interesting to note that for the three spatial structures, non-diagonal terms (d_{eff}^{xy} and d_{eff}^{yx}) can be neglected in comparison with the diagonal terms. In the case of the "dense" configuration, diagonal terms are equal ($d_{eff}^{xx} = d_{eff}^{yy}$). We can consider that the biofilm presents an isotropic behaviour in this case. In the case of "labyrinth" (respectively "worm-like") configuration, the

Author created version of the paper published in Journal of Biological Physics, Sept 2012, Volume 38, Issue 4, pp 573-588
Original publication available at http://link.springer.com, DOI: 10.1007%2Fs10867-012-9272-x

biofilm presents an orthotropic behaviour with an orthotropic coefficient equal to $\frac{d_{eff}^{xx}}{d_{eff}^{yy}} = 1.10$ (respectively 1.08). This orthotropic behaviour can also be explained by the mechanical pushing in the flow direction. Note that the diffusion in the x-direction is higher than the diffusion in the y-direction expressing a higher diffusion in the direction of the flow.

3.3 Sensitivity analysis of the ratio of the microscopic diffusions

In the precedent calculations, we have chosen $D_\sigma = 1\ \mu m^2.s^{-1}$ and $D_\beta = 100\ \mu m^2.s^{-1}$. However, it is very difficult to measure these values. In order to analyse the influence of these values, we perform a sensitivity analysis on the ratio of the subscellular parameters (D_σ / D_β). We have computed the effective diffusion d_{eff}^{xx} for four values of D_σ (0.1; 1; 5; 10) leading to four values of the ratio $\frac{D_\sigma}{D_\beta}$ (0.001; 0.01; 0.05; 0.1). The results are presented on Figure 8. The effective diffusion of "dense" configuration is lower than the effective diffusion of the "labyrinth" configuration which is lower than the "worm-like" configuration. This is because the bacteria density of the "dense" configuration is higher than the bacteria density of the "labyrinth" configuration which is higher than the density of the "worm-like" configuration.

In the "dense" configuration, the numerical results are very close to the Maxwell's model and to the Chang unit cell because the spatial structure is very close to a uniform distribution, which is the main hypothesis of these analytical solutions (see section 2.3). Moreover, the effective diffusion is very close to the bacteria diffusion because of a high density of bacteria.

Numerical results for the "worm-like" configuration present some differences with the analytical results. There is a shift between the models and numerical results are ranged between these models. However, there is a low nonlinearity because this configuration presents an

Author created version of the paper published in Journal of Biological Physics, Sept 2012, Volume 38, Issue 4, pp 573-588
Original publication available at http://link.springer.com, DOI: 10.1007%2Fs10867-012-9272-x

orthotropic behaviour. This curve remains enough close to the analytical solutions. It may be because the worm-like spatial structure is composed of uniformly distributed cell clusters. This uniform distribution can also be explained by the fact that the nutrient competition is very important with this configuration and consequently, small colonies remain enough distant from each other leading to this uniform distribution.

When computed numerically, the effective diffusion d_{eff}^{xx} of the "labyrinth" configuration is non linear with respect to the ratio $\frac{D_\sigma}{D_\beta}$. Indeed, this configuration presents privileged directions due to fingering and mechanical pushing which facilitate the substrate diffusion and create orthotropic behaviour. These directions affect drastically the calculation of the effective diffusion coefficients. This phenomenon is accentuated for low ratios because the diffusion process is high. The higher the ratio $\frac{D_\sigma}{D_\beta}$, the closer to the linearity is the curve because the effect of privileged directions decreases. Indeed, a ratio close to 1 leads to a homogeneous diffusion in the domain.

Note also that when the ratio $\frac{D_\sigma}{D_\beta}$, tends to 1, all curves reach a value of d_{eff}^{xx} equal to 100 $\mu m^2.s^{-1}$ because the diffusion tends to be homogeneous, which decreases the effect of the spatial structure.

These results have clearly shown that the spatial structure influences the nutrient diffusion. However, the reaction has to be considered to analyse the competition between growth and nutrient access. Indeed, the nutrient concentration widely influences the spatial structures (Xavier et al., 2009). The next section focuses on substrate consumption using Monod equation.

Author created version of the paper published in Journal of Biological Physics, Sept 2012, Volume 38, Issue 4, pp 573-588
Original publication available at http://link.springer.com, DOI: 10.1007%2Fs10867-012-9272-x

3.4 Calculation of the substrate consumption ratio

As explained above, experimental spatial structures have been obtained by varying the nutrient concentration (Xavier et al., 2009). In this section, we investigate the influence of the initial solute concentration c_0 on the substrate consumption ratio. For this purpose, we consider that diffusion-reaction phenomena are present in the bacteria clusters. There is no reaction term elsewhere. Considering the reaction term *R* leads to:

$$\underbrace{\nabla.(D_\sigma \nabla c_\sigma)}_{diffusion} = \underbrace{R}_{reaction}, \quad in\Omega_\sigma \tag{22}$$

and

$$\underbrace{\nabla.(D_\beta \nabla c_\beta)}_{diffusion} = 0, \quad in\Omega_\beta \tag{23}$$

The reaction term R (mol.µm^{-3}.s^{-1}) is expressed following a Monod equation (Kreft et al., 2001; Monod, 1942; Picioreanu et al., 2004):

$$R = \mu * \rho_\sigma * \frac{c_\sigma}{c_\sigma + ks} \tag{24}$$

where μ =1 s^{-1} and *ks* =0.5 mol.µm^{-3}. The coefficient µ represents the maximum growth rate coefficient expressed in s^{-1}, ρ_σ the biomass density expressed in mol.µm^{-3} and *ks* is the Monod coefficient expressed in mol.µm^{-3}. This is also called the half-saturation coefficient because it corresponds to the concentration at which is one-half of its maximum. We can assess the macroscopic substrate consumption c_{sub} as follows:

$$c_{sub} = \frac{1}{\Omega}\int_\Omega c d\Omega \tag{25}$$

The diffusion parameters are the same as the parameters used in section 3.2. Initial conditions

Author created version of the paper published in Journal of Biological Physics, Sept 2012, Volume 38, Issue 4, pp 573-588
Original publication available at http://link.springer.com, DOI: 10.1007%2Fs10867-012-9272-x

are: $c(L_1) = c(L_2) = c(L_3) = c(L_4) = c_0$. Figure 9 presents the calculation of the macroscopic substrate consumption c_{sub} with respect to the initial solute concentration c_0 for the three configurations.

For $c_0 < 1$ mol.μm^{-3}, nutrient competition between bacteria is very important, biofilm growth is therefore difficult, small colonies form the biofilm. The "worm-like" configuration presents the higher value of consumption ratio in the case of low initial substrate concentration. Moreover, the "dense" configuration has the lowest substrate consumption. We can conclude that the "worm-like" configuration is optimal for low values of c_0. It also corresponds to the results observed in experimental studies where the growth is limited by the nutrient access.

For $1 < c_0 < 100$ mol.μm^{-3}, the nutrient concentration is too low to generate a dense biofilm but high enough to heterogeneously feed bacteria. In this case, the "labyrinth" configuration presents a higher substrate consumption than the "worm-like" configuration despite a higher density. We can conclude, in this range of values of c_0, that the "labyrinth" configuration is the most appropriate configuration. It is the optimal organization when the competition between growth and nutrient access is important as observed in experimental studies.

For $c_0 > 100$ mol.μm^{-3}, the substrate concentration is high, there is no competition between cells. In this case, the initial concentration c_0 is sufficient to feed all bacteria. The substrate consumption ratio is therefore the highest with the "dense" configuration. We can conclude that, with a saturated substrate concentration, the biofilm growth is maximal with a "dense" configuration.

These results strengthen the experience of Joao & al. and therefore explain the continuity in term of spatial structures obtained by increasing the initial substrate concentration (see Figure 1).

Author created version of the paper published in Journal of Biological Physics, Sept 2012, Volume 38, Issue 4, pp 573-588
Original publication available at http://link.springer.com, DOI: 10.1007%2Fs10867-012-9272-x

4 Conclusion

The competition between growth and nutrient access plays a major role in the emergence of different biofilm spatial structures and this variety of spatial structures leads to different physical properties of the biofilm. In order to explore more deeply this phenomenon, we have proposed a numerical procedure investigating the impact of spatial structures on the effective diffusion and on the substrate consumption ratio. We have applied this procedure on three kinds of spatial structure. The results have shown that the effective diffusion depends on the spatial structure of the RVE, the subcellular-scale parameters (D_σ and D_β) and also the bacterial density in the RVE.

With the "dense" configuration, the nutrient concentration is important, there is no competition between growth and nutrient access, all bacteria have an important nutrient access, the growth is maximal and the diffusion process has therefore a minor role. The results are very close to the analytical solutions.

On the contrary, with the "worm-like" configuration, the nutrient concentration is limited, the competition between growth and nutrient access is therefore very important. The biofilm is composed of small colonies, the diffusion process has a major role.

The "labyrinth" configuration is an intermediate step, the biofilm growth is heterogeneous. Mechanical pushing and fingering lead to this configuration because of the competition between growth and nutrient access. The labyrinth configuration has shown a good compromise between the diffusion and the substrate consumption.

The calculation of effective diffusion coefficients has shown an orthotropic behaviour of the structures in the case of "worm-like" and "labyrinth" configurations. In these cases, the mechanical pushing and the fingering lead to a configuration with privileged directions and to higher values of effective diffusion in the direction of the flow. This orthotropic behaviour

Author created version of the paper published in Journal of Biological Physics, Sept 2012, Volume 38, Issue 4, pp 573-588
Original publication available at http://link.springer.com, DOI: 10.1007%2Fs10867-012-9272-x

explains the non linear evolution of the effective diffusion following the microscopic diffusion coefficients.

It is interesting to note that the conclusions of Xavier & al. (Xavier et al., 2009) in terms of nutrient competition and biofilm growth clearly correspond to these results in terms of effective diffusion and substrate consumption ratio. We have provided a link between nutrient competition, biofilm growth and effective diffusion in the spatial structure of bacterial biofilms.

Moreover, this study has highlighted the importance of the bacteria density on the calculation of effective diffusion coefficients and on the substrate consumption ratio. It seems to be interesting to compare the value of effective diffusion of spatial structures with the same density in order to clearly distinguish the effect of the spatial structure and the effect of the density.

Acknowledgment

This work was supported in part by the project ANR DISCO (ANR DISCO 09-SYSC-003, SYSCOMM call). The first author's work is carried out at the French Regional Council of Auvergne. This publication only reflects the authors' view.

Author created version of the paper published in Journal of Biological Physics, Sept 2012, Volume 38, Issue 4, pp 573-588
Original publication available at http://link.springer.com, DOI: 10.1007%2Fs10867-012-9272-x

References:

Allesen-Holm, M., Barken, K., Yang, L., Klausen, M.,Webb, J., Kjelleberg, S., Molin, S., Givskov, M., and Tolker-Nielsen, T. (2006). A characterization of dna release in pseudomonas aeruginosa cultures and biofilms. Molecular Microbiology, 59(4):1114-1128.

Bakken, L. and Olsen, R. (1983). Buoyant densities and dry-matter contents of microorganisms: Conversion of a measured biovolume into biomass. Applied and Environmental Microbiology, 45(4):1188-1195.

Beech, I. and Sunner, J. (2004). Biocorrosion: Towards understanding interactions between biofilms and metals. Current Opinion in Biotechnology, 15(3):181-186.

Beyenal, H. and Tanyolac, A. (1994). The calculation of simultaneous effective diffusion coefficients of the substrates in a fluidized bed biofilm reactor. Water Science and Technology, 29(10-11):463-470.

Bratbak, G. and Dundas, I. (1984). Bacterial dry matter content and biomass estimations. Applied and Environmental Microbiology, 48(4):755-757.

Chang, H.-C. (1983). Effective diffusion and conduction in two-phase media: A unified approach. AIChE Journal, 29(5):846-853.

Costerton, J., Lewandowski, Z., Caldwell, D., Korber, D., and Lappin-Scott, H. (1995). Microbial biofilms. Annual Review of Microbiology, 49:711-745.

Daims, H., Nielsen, P., Nielsen, J., Juretschko, S., and Wagner, M. (2000). Novel nitrospira-like bacteria as dominant nitrite-oxidizers in biofilms from wastewater treatment plants: Diversity and in situ physiology. Water Science and Technology, 41(4-5):85-90.

De Beer, D., Stoodley, P., and Lewandowski, Z. (1997). Measurement of local diffusion coefficients in biofilms by microinjection and confocal microscopy. Biotechnology and Bioengineering, 53(2):151-158.

De Beer, D., Stoodley, P., Roe, F., and Lewandowski, Z. (1994). Effects of biofilm structures on oxygen distribution and mass transport. Biotechnology and Bioengineering, 43(11):1131-1138.

Dibdin, G. (1981). Diffusion of sugars and carboxylic acids through human dental plaque in vitro. Archives of Oral Biology, 26(6):515-523.

Dockery, J. and Klapper, I. (2002). Finger formation in biofilm layers. SIAM Journal on Applied Mathematics, 62(3):853-869.

Donlan, R. and Costerton, J. (2002). Biofilms: Survival mechanisms of clinically relevant microorganisms. Clinical Microbiology Reviews, 15(2):167-193.

Fan, L.-S., Leyva-Ramos, R., Wisecarver, K., and Zehner, B. (1990). Diffusion of phenol through a biofilm grown on activated carbon particles in draft-tube three-phase fluidized-bed bioreactor. Biotechnology and Bioengineering, 35(3):279-286.

Gujer, W. and Wanner, O. (1990). Modeling mixed population biofilms, in Biofilms, characklis, w.g. and marshall (eds.), wiley, new york, usa.

Hashin, Z. (1983). Analysis of composite materials - a survey. Journal of Applied Mechanics, Transactions ASME, 50(3):481-505.

Hunter, R. and Beveridge, T. (2005). High-resolution visualization of pseudomonas aeruginosa pao1 biofilms by freeze-substitution transmission electron microscopy. Journal of Bacteriology, 187(22):7619-7630.

Jefferson, K. (2004). What drives bacteria to produce a biofilm? FEMS Microbiology Letters, 236(2):163-173.

Kreft, J.-U., Picioreanu, C., Wimpenny, J., and Van Loosdrecht, M. (2001). Individual-based modelling of biofilms. Microbiology, 147(11):2897-2912.

La Cour Jansen, J. and Harremoes, P. (1985). Removal of soluble substrates in fixed films. Water Science and Technology, 17(2-3 -3 pt 1):1-14.

Lamotta, E. (1976). Internal diffusion and reaction in biological films. Environmental Science and Technology, 10(8):765-769.

Libicki, S. B., Salmon, P. M., and Robertson, C. R. (1988). Effective diffusive permeability of a nonreacting solute in microbial cell aggregates. Biotechnology and Bioengineering, 32(1):68-85.

Mathias, J.-D. and Tessier-Doyen, N. (2008). Homogenization of glass/alumina two-phase materials using a cohesive zone model. Computational Materials Science, 43(4):1081-1085.

Matson, J. and Characklis, W. (1976). Diffusion into microbial aggregates. Water Research, 10(10):877-885.

Monod, J. (1942). Recherches sur la croissance des cultures bacteriennes.

Ochoa, J., Stroeve, P., and Whitaker, S. (1986). Diffusion and reaction in cellular media. Chemical Engineering Science, 41(12):2999-3013.

Ochoa-Tapia, J., Stroeve, P., and Whitaker, S. (1994). Diffusive transport in two-phase media: spatially periodic models and maxwell's theory for isotropic and anisotropic systems. Chemical Engineering Science, 49(5):709-726.

Pamp, S. and Tolker-Nielsen, T. (2007). Multiple roles of biosurfactants in structural biofilm development by pseudomonas aeruginosa. Journal of Bacteriology, 189(6):2531-2539.

Picioreanu, C., Kreft, J.-U., and Van Loosdrecht, M. (2004). Particle-based multidimensional multispecies biofilm model. Applied and Environmental Microbiology, 70(5):3024-3040.

Rieu, A., Briandet, R., Habimana, O., Garmyn, D., Guzzo, J., and Piveteau, P. (2008). Listeria monocytogenes egde biofilms: No mushrooms but a network of knitted chains. Applied and Environmental Microbiology, 74(14):4491-4497.

Roszak, D. and Colwell, R. (1987). Survival strategies of bacteria in the natural environment. Microbiological Reviews, 51(3):365-379.

Stewart, P. (1998). A review of experimental measurements of effective diffusive permeabilities and effective diffusion coefficients in biofilms. Biotechnology and Bioengineering, 59(3):261-272.

Stewart, P. and Costerton, J. (2001). Antibiotic resistance of bacteria in biofilms. Lancet, 358(9276):135-138.

Thar, R. and Kuhl, M. (2005). Complex pattern formation of marine gradient bacteria explained by a simple computer model. FEMS Microbiology Letters, 246(1):75-79.

Tijhuis, L., Van Loosdrecht, M., and Heijnen, J. (1994). Formation and growth of heterotrophic aerobic biofilms on small suspended particles in airlift reactors. Biotechnology and Bioengineering, 44(5):595-608.

Wanner, O. and Reichert, P. (1996). Mathematical modeling of mixed-culture biofilms. Biotechnology and Bioengineering, 49(2):172-184.

Wood, B., Quintard, M., and Whitaker, S. (2001). Methods for predicting diffusion coefficients in biofilms and cellular systems. Methods in Enzymology, 337:319-338.

Wood, B., Quintard, M., and Whitaker, S. (2002). Calculation of effective diffusivities for biofilms and tissues. Biotechnology and Bioengineering, 77(5):495-516.

Wood, B. and Whitaker, S. (1998). Diffusion and reaction in biofilms. Chemical Engineering Science, 53(3):397-425.

Xavier, J., Martinez-Garcia, E., and Foster, K. (2009). Social evolution of spatial patterns in bacterial biofilms: When conflict drives disorder. American Naturalist, 174(1):1-12.

Author created version of the paper published in Journal of Biological Physics, Sept 2012, Volume 38, Issue 4, pp 573-588
Original publication available at http://link.springer.com, DOI: 10.1007%2Fs10867-012-9272-x

List of figure captions

Figure 1: Example of different biofilm patterns Xavier20091.
Figure 2: Schematic description of the homogenization process.
Figure 3: Subcellular-scales.
Figure 4: Numerical flowchart.
Figure 5: Boundary conditions for the RVE.
Figure 6: RVE convergence: different sizes have to be tested in order to determine the suitable size.
Figure 7: Convergence study.
Figure 8: Sensitivity analysis.
Figure 9: Variation of the substrate consumption ratio.

Author created version of the paper published in Journal of Biological Physics, Sept 2012, Volume 38, Issue 4, pp 573-588
Original publication available at http://link.springer.com, DOI: 10.1007%2Fs10867-012-9272-x

List of Figures

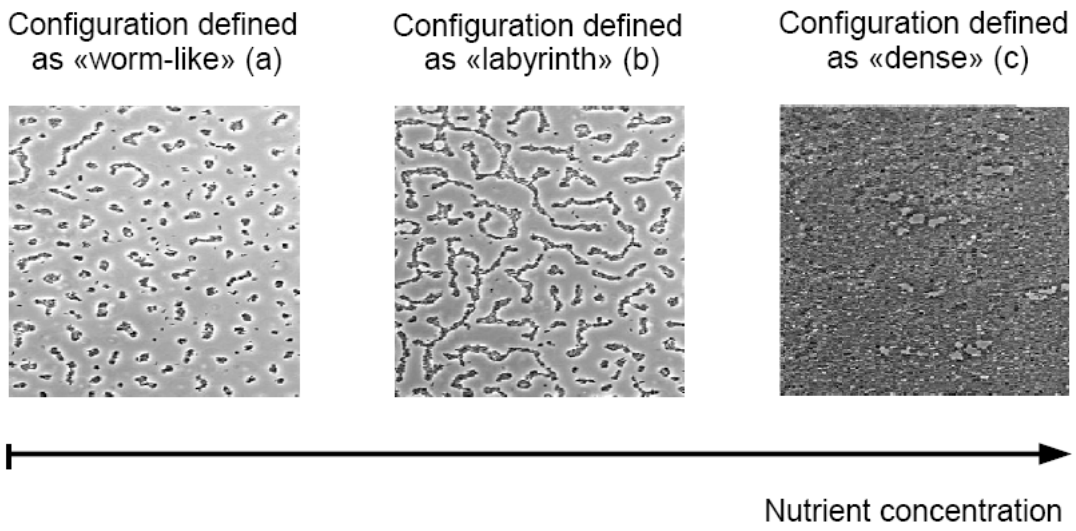

Figure 1: Example of different biofilm patterns (Xavier et al., 2009)

Author created version of the paper published in Journal of Biological Physics, Sept 2012, Volume 38, Issue 4, pp 573-588
Original publication available at http://link.springer.com, DOI: 10.1007%2Fs10867-012-9272-x

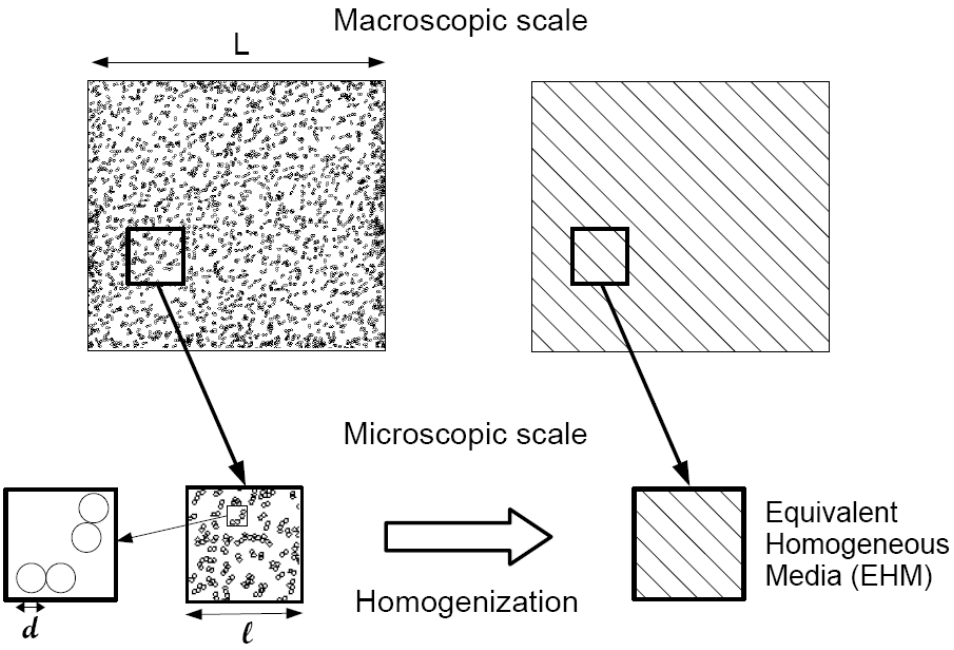

Figure 2: Schematic description of the homogenization process

Author created version of the paper published in Journal of Biological Physics, Sept 2012, Volume 38, Issue 4, pp 573-588
Original publication available at http://link.springer.com, DOI: 10.1007%2Fs10867-012-9272-x

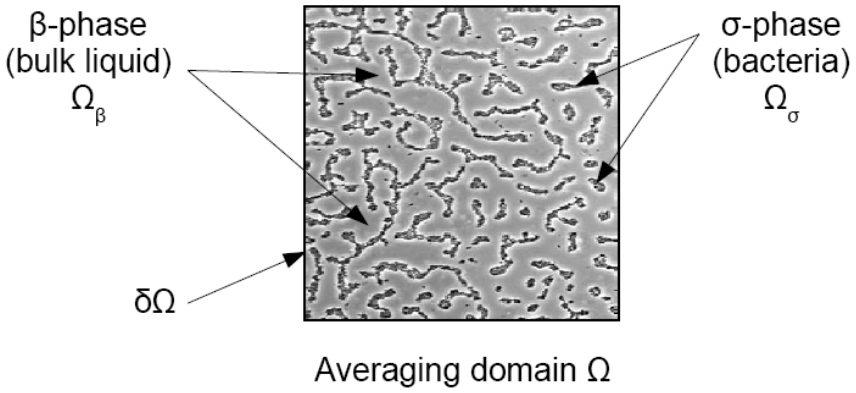

Figure 3: Subcellular-scales

Author created version of the paper published in Journal of Biological Physics, Sept 2012, Volume 38, Issue 4, pp 573-588
Original publication available at http://link.springer.com, DOI: 10.1007%2Fs10867-012-9272-x

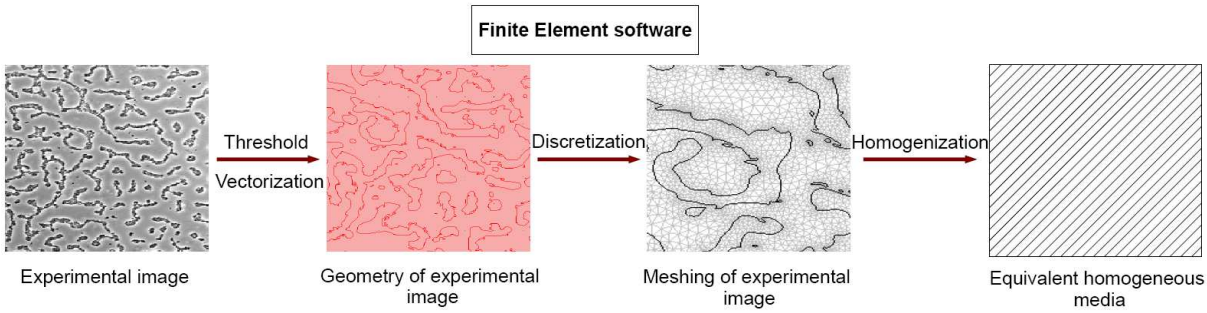

Figure 4: Numerical flowchart

Author created version of the paper published in Journal of Biological Physics, Sept 2012, Volume 38, Issue 4, pp 573-588
Original publication available at http://link.springer.com, DOI: 10.1007%2Fs10867-012-9272-x

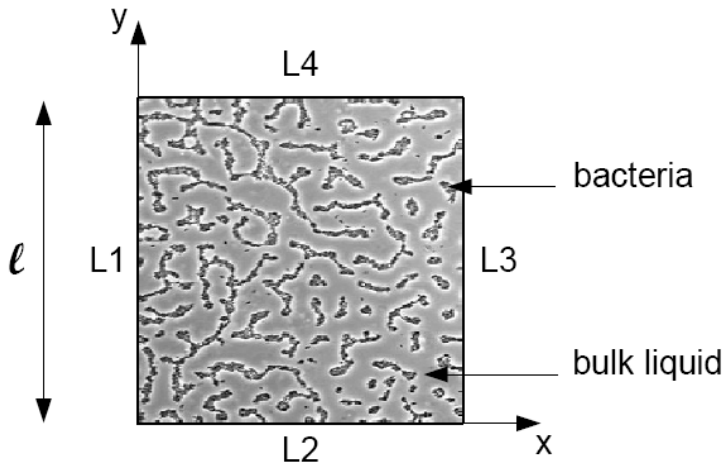

Figure 5: Boundary conditions for the RVE

Author created version of the paper published in Journal of Biological Physics, Sept 2012, Volume 38, Issue 4, pp 573-588
Original publication available at http://link.springer.com, DOI: 10.1007%2Fs10867-012-9272-x

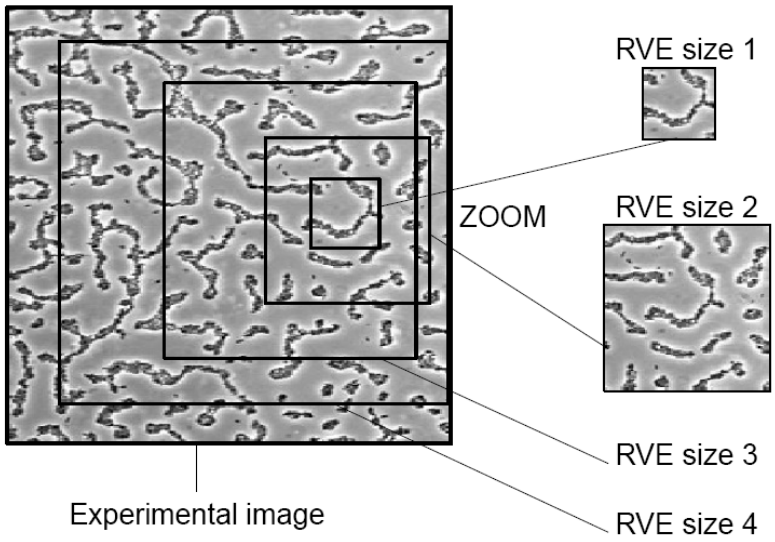

Figure 6: RVE convergence: different sizes have to be tested in order to determine the suitable size.

Author created version of the paper published in Journal of Biological Physics, Sept 2012, Volume 38, Issue 4, pp 573-588
Original publication available at http://link.springer.com, DOI: 10.1007%2Fs10867-012-9272-x

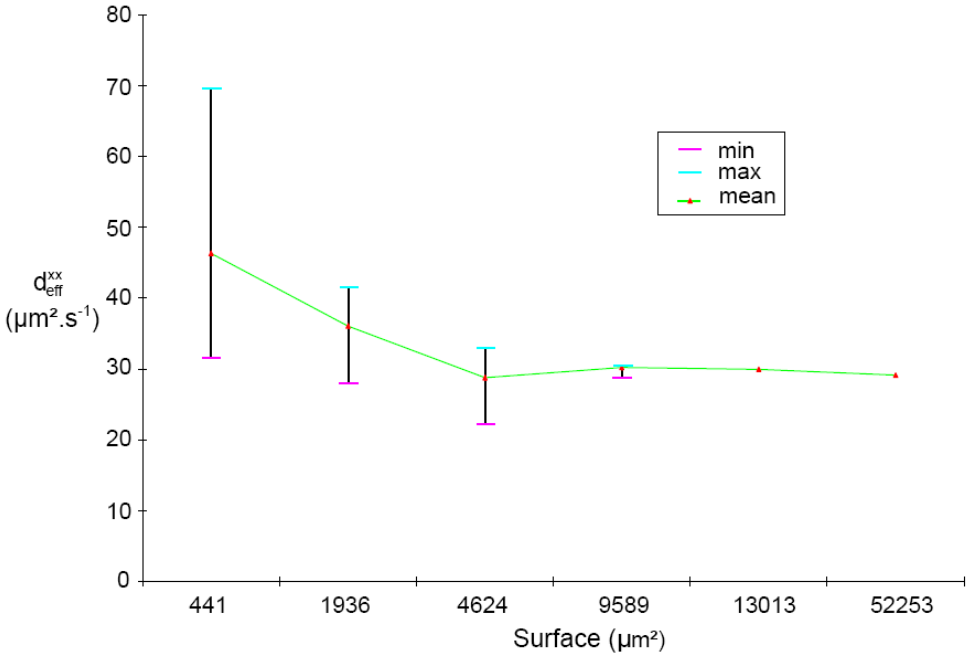

Figure 7: Convergence study

Author created version of the paper published in Journal of Biological Physics, Sept 2012, Volume 38, Issue 4, pp 573-588
Original publication available at http://link.springer.com, DOI: 10.1007%2Fs10867-012-9272-x

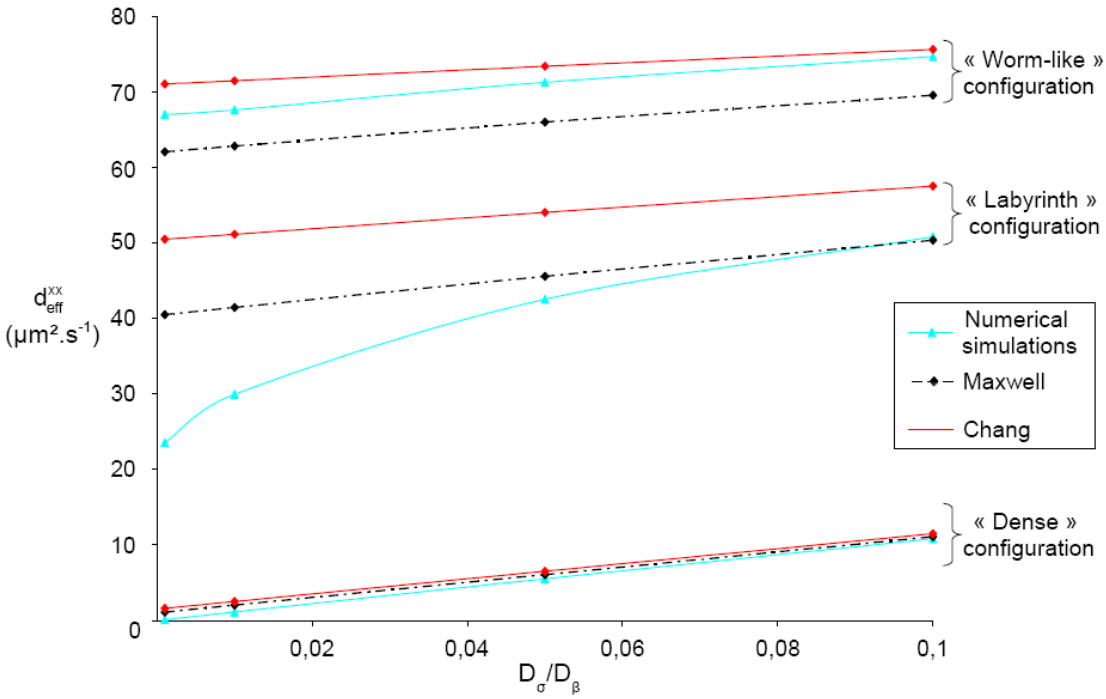

Figure 8: Sensitivity analysis

Author created version of the paper published in Journal of Biological Physics, Sept 2012, Volume 38, Issue 4, pp 573-588
Original publication available at http://link.springer.com, DOI: 10.1007%2Fs10867-012-9272-x

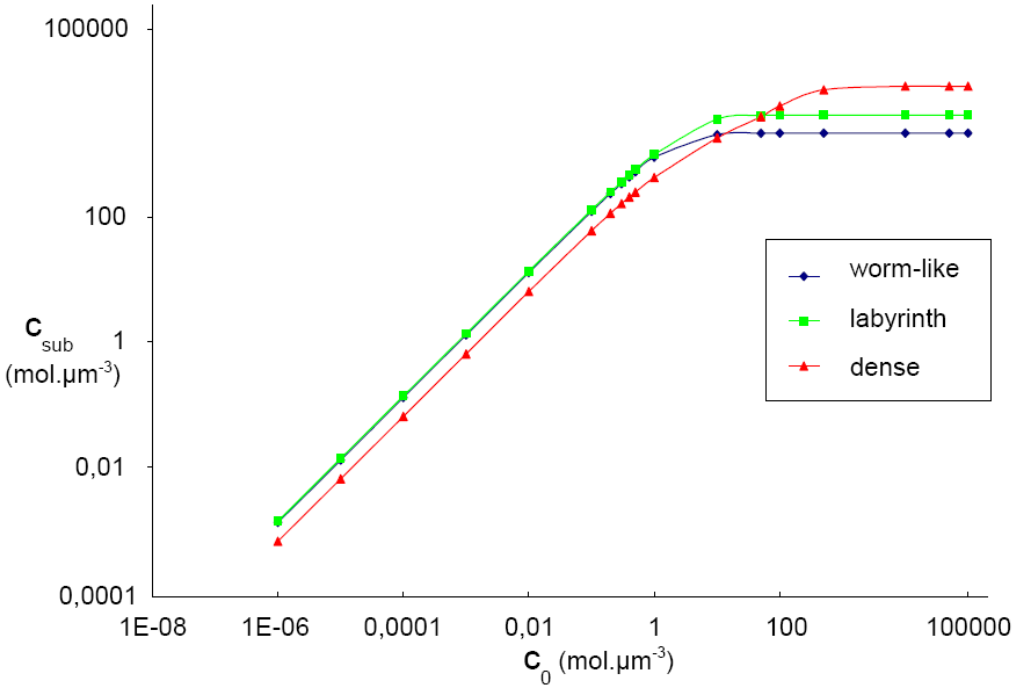

Figure 9: Variation of the substrate consumption ratio